

η MAID-2015: update with new data and new resonances

V.L. Kashevarov, L. Tiator, M. Ostrick
 Institut für Kernphysik, Johannes Gutenberg-Universität
 D-55099 Mainz, Germany

June 22, 2021

Abstract

Recent data for η and η' photoproduction on protons obtained by the A2 Collaboration at MAMI are presented. The total cross section for η photoproduction demonstrates a cusp at the energy corresponding to the η' threshold. The new data and existing data from GRAAL, CBELSA/TAPS, and CLAS collaborations have been analyzed by an expansion in terms of associated Legendre polynomials. The isobar model η MAID updated with η' channel and new resonances have been used to fit the new data. The new solution η MAID-2015 reasonably good describes the data in the photon beam energy region up to 3.7 GeV.

1 Introduction

The unitarity isobar model η MAID [1] was developed in 2002 for η photo- and electroproduction on nucleons. The model includes a nonresonant background, which consists of nucleon Born terms in the s and u channels and the vector meson exchange in the t channel, and s -channel resonance excitations. The Born terms are evaluated with the pseudoscalar coupling. The vector meson contribution is obtained by the ρ and ω meson exchange in the t channel with pole-like Feynman propagators. For each partial wave the resonance contribution is parameterized by the Breit-Wigner function with energy dependent widths. The η MAID-2003 version includes 8 resonances, $N(1520)3/2^-$, $N(1535)1/2^-$, $N(1650)1/2^-$, $N(1675)5/2^-$, $N(1680)5/2^+$, $N(1700)3/2^-$, $N(1710)1/2^+$, $N(1720)3/2^+$, and was fitted to proton data for differential cross sections and beam asymmetry at photon beam energies up to 1400 MeV. The η MAID-2003 version describes not only the experimental data available in 2002, but even a bump structure around $W=1700$ MeV in η photoproduction on the neutron, which was observed a few years later. However, this version fails to reproduce the new polarization data obtained in Mainz [2].

The aim of this work is to extend the η MAID-2003 version to higher energies, to improve a description of the new polarization data, and to include the η' photoproduction channel.

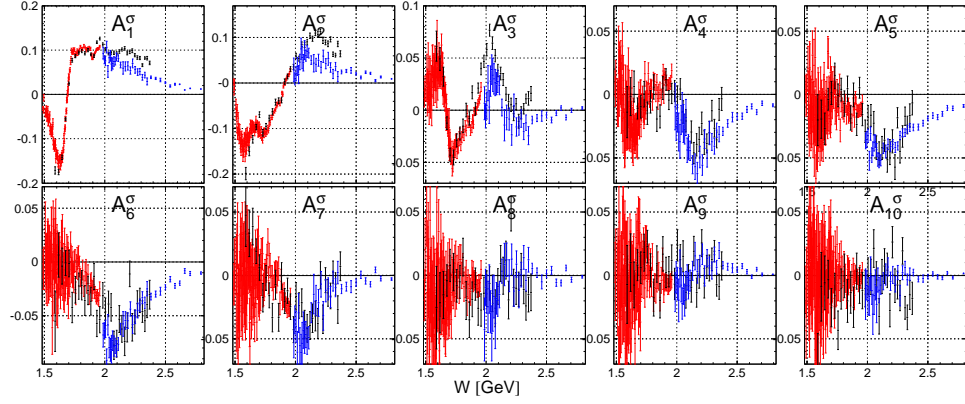


Figure 1: Legendre coefficients in $[\mu b/sr]$ up to $\ell_{\max} = 5$ from our fits to the differential cross section of the $\gamma p \rightarrow \eta p$ reaction as function of the center-of-mass energy W . Red circles are fit results for preliminary A2MAMI data [3], black and blue - for CBELSA/TAPS [4] and CLAS [5] data correspondingly.

2 Truncated Legendre analysis

The full angular coverage of differential cross sections and polarization observables allow us to perform a fit with a Legendre series truncated to a maximum orbital angular momentum ℓ_{\max} :

$$\frac{d\sigma}{d\Omega} = \sum_{n=0}^{2\ell_{\max}} A_n^{\sigma} P_n^0(\cos \Theta_{\eta}), \quad (1)$$

$$T(F) \frac{d\sigma}{d\Omega} = \sum_{n=1}^{2\ell_{\max}} A_n^{T(F)} P_n^1(\cos \Theta_{\eta}), \quad (2)$$

$$\Sigma \frac{d\sigma}{d\Omega} = \sum_{n=2}^{2\ell_{\max}} A_n^{\Sigma} P_n^2(\cos \Theta_{\eta}), \quad (3)$$

where $P_n^m(\cos \Theta_{\eta})$ are associated Legendre polynomials. The spin-dependent cross sections, $Td\sigma/d\Omega$, $Fd\sigma/d\Omega$, and $\Sigma d\sigma/d\Omega$ were obtained by multiplying the corresponding asymmetries with the differential cross sections obtained in Mainz. As an example, the results for the Legendre coefficients for differential cross sections are presented in Figs. 1 and 2. A non-zero A_{10} only possible with h -wave contribution, A_9 is dominated by the an interference between g and h waves, A_8 includes g , h waves and an interference between f and h waves, and so on. The first coefficient, A_0 , was omitted in the figures because of it includes all possible partial-wave amplitudes and just only reflects the magnitude of the total cross section, see Fig. 3.

Non-zero values of the A_7 and A_8 coefficients point to a contribution of the g wave at energies above $W=2$ GeV for both η and η' channels. The errors in the determination of the coefficients A_9 and A_{10} do not allow any conclusions about the contribution of h wave in these reactions. Polarization observables for η photoproduction were measured below $W=1.9$ GeV. The Legendre fit for these data shows the sensitivity to small partial-wave contributions and indicates pd interferences below $W=1.6$ GeV and df interferences above $W=1.6$ GeV [2].

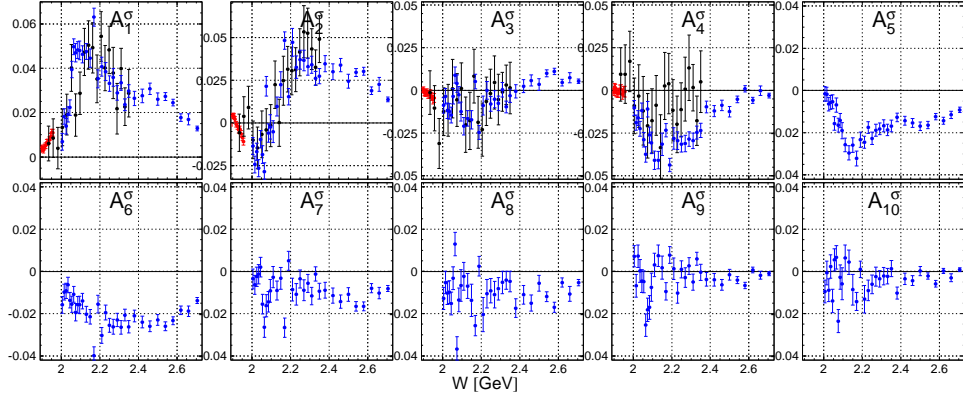


Figure 2: The same as Fig. 1, but for the $\gamma p \rightarrow \eta' p$ reaction.

3 Updated η MAID

New η MAID-2015 model is based on the η MAID-2003 version. The following main changes were made:

- 12 additional resonances were added: $N(1860)5/2^+$, $N(1875)3/2^-$, $N(1880)1/2^+$, $N(1895)1/2^-$, $N(1900)3/2^+$, $N(1990)7/2^+$, $N(2000)5/2^+$, $N(2060)5/2^-$, $N(2120)3/2^-$, $N(2190)7/2^-$, $N(2220)9/2^+$, and $N(2250)9/2^-$;
- electromagnetic couplings for the vector mesons were updated according to Ref. [6];
- hadronic vector and tensor couplings for the vector mesons were fixed from Ref. [7];
- data base for the fit was updated.

The new model was fitted to data of differential cross sections from A2MAMI [3] and CLAS Collaborations [5], polarisation observables T, F [2] and Σ [8], [9]. The main variable parameters for each resonance: Breit-Wigner mass, total width, branching ratio to ηp (or $\eta' p$) decay, photoexcitation helicity amplitudes $A_{1/2}$ and $A_{3/2}$, a relative sign between the $N^* \rightarrow \eta N$ and the $N^* \rightarrow \pi N$ couplings. Besides, the hadronic pseudoscalar coupling for the Born term contribution, cutoffs for dipole formfactors of the vector mesons, damping factors for the partial widths and the electromagnetic form factor of the resonances were also fitted. Branching ratios for hadronic decays of the resonances besides the investigated channel were fixed.

As an initial parameter set for the Breit-Wigner parameters the last BnGa solution [10] was used. As initial parameter limits uncertainties from Refs. [6] and [10] were used. As the first step, for each resonance $A_{1/2}$ and $A_{3/2}$ are fixed because of a strong correlation with the branching ratio. On the second step the branching ratios obtained on the first step are fixed, but $A_{1/2}$ and $A_{3/2}$ are variable, and so on. After few iterations the initial limits are changed if necessary. The fits for the η and η' channels were done independently.

The fit results for the total cross sections and the polarization observables are presented in Figs. 3-6 together with corresponding experimental data. We used the differential cross section from the CLAS Collaboration [5] in this fit because of their much smaller statistical errors, larger energy covering, and better agreement with the high statistic data from A2MAMI [3] in an overlapping energy region. Unfortunately, the total cross section was

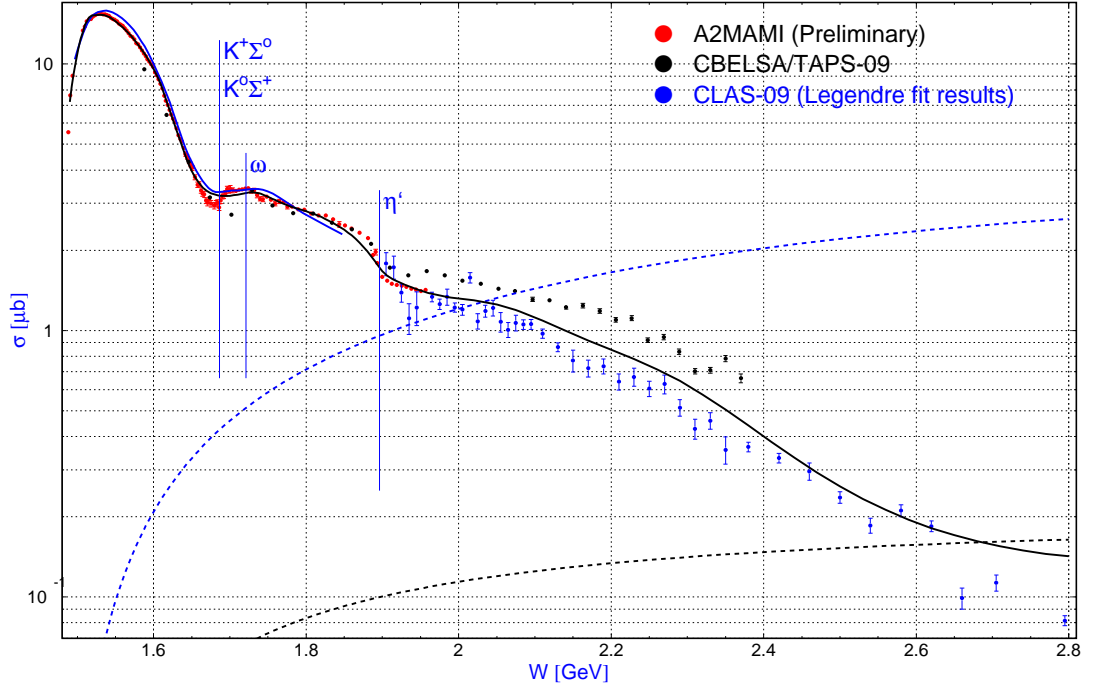


Figure 3: Total cross section of the $\gamma p \rightarrow \eta p$ reaction. Solid blue curve is η MAID-2003 isobar model [1], black solid curve: new η MAID-2015 solution. Prediction of η MAID-2003 for background contribution is shown by blue dashed line, background of η MAID-2015 - black dashed line. Vertical lines correspond to thresholds of $K\Sigma$, ω , and η' photoproductions.

not determined in Ref. [5] and we calculated it using Legendre decomposition for the differential cross sections. Blue circles in Figs. 3 and 5 are results of this procedure.

In Fig. 3, there is a very interesting feature at energy ~ 1900 MeV, which could be explained by a cusp due to the opening of a new channel, η' photoproduction. The main resonance, which is responsible for this effect is the $N(1895)1/2^-$. The Breit-Wigner parameters of this state were determined by the fit as following: $M = 1896 \pm 1$ MeV, $\Gamma_{tot} = 93 \pm 13$ MeV, $\Gamma_{\eta p} = (14 \pm 3)\%$, $\Gamma_{\eta' p} = (6.5 \pm 2)\%$, and $A_{1/2} = (-17.4 \pm 1.5)10^{-3} GeV^{-1/2}$. Fig. 4 demonstrates a significant improvement of description for T and F asymmetries (red lines) in comparison with the η MAID-2003 version (blue lines).

A very good agreement with the experimental data was obtained for the cross section of the $\gamma p \rightarrow \eta' p$ reaction (see Fig. 5). The main contributions to this reaction come from $N(1895)1/2^-$, $N(1900)3/2^+$, $N(1880)1/2^+$, $N(2150)3/2^-$, and $N(2000)5/2^+$ resonances. Other resonance contributions are much smaller than the background. The new η MAID-2015 solution describes shape of the GRAAL data for Σ near threshold, but not the magnitude (see Fig. 6). To explain, why the magnitude of the asymmetry is larger at lower energy, it is probably necessary to include below threshold resonances using the more realistic approach applied in Ref. [11] for the Roper resonance at η -meson photoproduction.

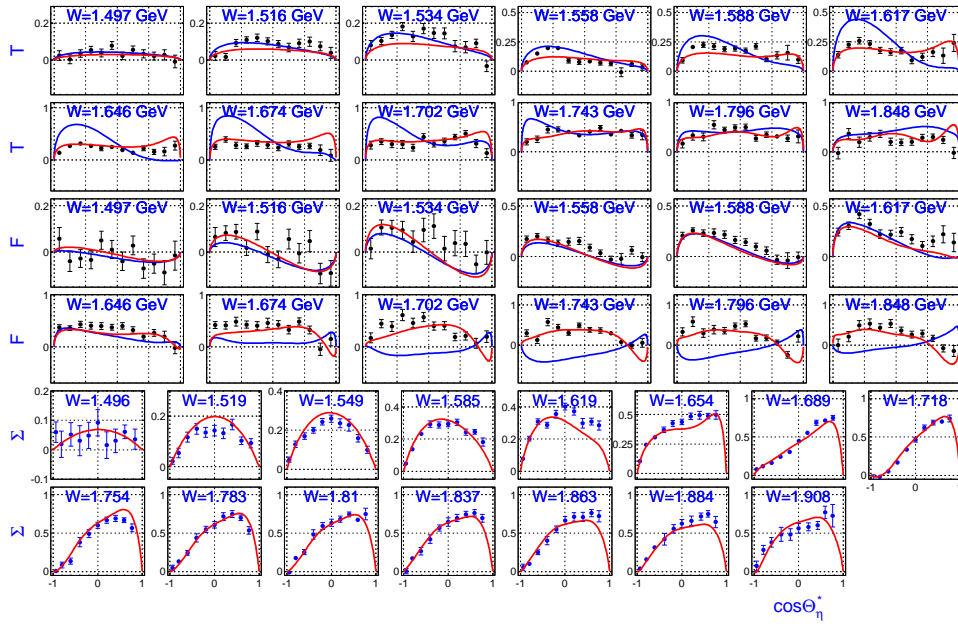


Figure 4: η MAID-2015 solution for the η channel (red lines). Black circles: A2MAMI-15 data [2] for T and F asymmetries, blue circles: GRAAL-07 data [8] for Σ . Blue lines: η MAID-2003 prediction [1].

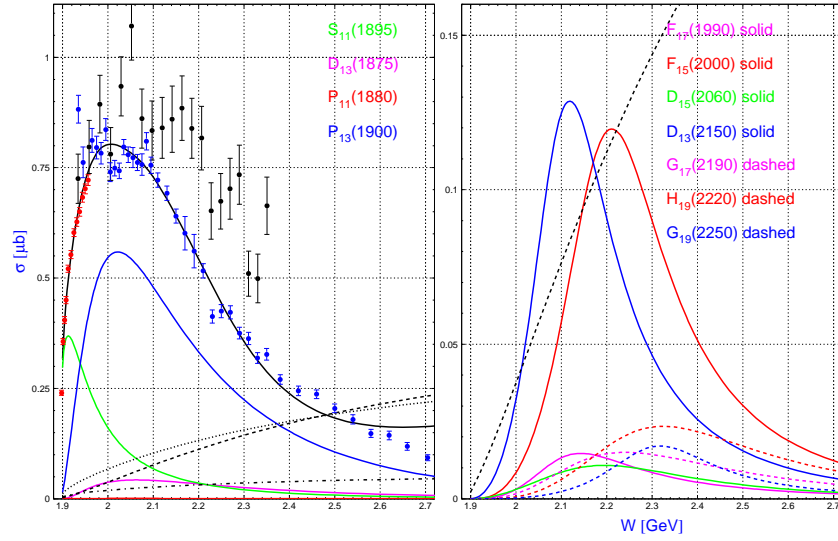


Figure 5: Total cross section of the $\gamma p \rightarrow \eta p$ reaction. Red circles: A2MAMI-15 data [3], black circles: CBELSA/TAPS-09 [4], blue circles: data obtained from the Legendre fit to the differential cross sections of the CLAS Collaboration [5]. Solid black line: η MAID-2015 solution. Background contribution is shown by dashed black line. Black dotted and dot-dashed lines are partial contributions of the Born terms and the vector mesons correspondingly. Other curves are partial contributions of resonances.

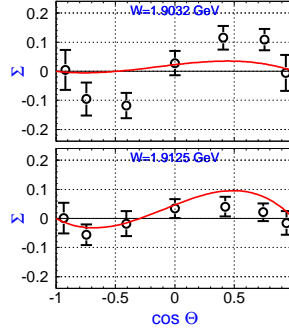


Figure 6: Beam asymmetry Σ . Data from Ref.[9], red curves are η MAID-2015 solution.

4 Summary and conclusions

In summary, we have presented new version η MAID-2015. The model describes available data for the $\gamma p \rightarrow \eta p$ and $\gamma p \rightarrow \eta' p$ reactions reasonably well. The cusp at $W \sim 1900$ MeV in $\gamma p \rightarrow \eta p$ reaction was explained as a threshold effect from the η' channel. Parameters of $N(1895)1/2^-$ resonance, responsible for this effect, were determined. A further improvement could be achieved by adding below threshold resonances and using Regge trajectories for the vector mesons in t channel. Furthermore, polarization observables which should come soon from A2MAMI, CBELSA/TAPS, and CLAS Collaborations will help to improve the model.

This work was supported by the Deutsche Forschungsgemeinschaft (SFB 1044).

References

- [1] W. -T. Chiang, S. N. Yang, L. Tiator, and D. Drechsel, Nucl. Phys. **A700**, 429 (2002).
- [2] J. Akondi *et al.* (A2 Collaboration at MAMI), Phys. Rev. Lett. **113**, 102001 (2014).
- [3] P. Adlarson *et al.* (A2 Collaboration at MAMI), Submitted to Phys. Rev. Lett.
- [4] V. Crede *et al.* (CBELSA/TAPS Collaboration), Phys. Rev. C **80**, 055202 (2009).
- [5] M. Williams *et al.* (CLAS Collaboration), Phys. Rev. C **80**, 045213 (2009).
- [6] K. A. Olive *et al.* (Particle Data Group), Chin. Phys. C **38**, 090001 (2014).
- [7] J. M. Laget *et al.*, Phys. Rev. C **72**, 022202(R) (2005).
- [8] O. Bartalini *et al.* (The GRAAL Collaboration), Eur. Phys. J. A **33**, 169 (2007).
- [9] G. Mandaglio *et al.*, EPJ Web of Conferences **72** 00016 (2014); P. Levi Sandri *et al.*, arXiv:1407.6991v2.
- [10] A. V. Anisovich, R. Beck, E. Klempt, V. A. Nikonov, A. V. Sarantsev, U. Thoma, Eur. Phys. J. A **48**, 15 (2012).
- [11] I. G. Aznauryan, Phys. Rev. C **68**, 065204 (2003).